NOTATION

φ, r, z, cylindrical coordinates; x, y, z, Cartesian coordinates; H and S, channel depth and width; δ, lead angle of the spiral; ω_0, angular velocity of the smooth disk; r_i, r, r_0, inside radius, the radius at any given point, and the outside radius of the spiral along its median line; $A\varphi$, A_r, A_x, A_y, pressure gradients; ρ, density of the fluid; c_1 and c_2, integration constants; $\tau\varphi z$, τrz, τxz, τyz, components of the stress tensor; $V\varphi$, V_r, V_x, V_y, projections of the velocity of the fluid on the axes φ, r, x, y, respectively; τ, stress deviator; B and n, rheological parameters; Δ, strain rate tensor; V_1, V_2, V_3, V_4, dimensionless velocities of the fluid; a, ratio of pressure gradients; Q_x and Q_y, true flow rates in the directions x and y, respectively; $Q_{x,max}$, true flow rate corresponding to a zero pressure head; q_x and q_y, dimensionless flow rates; l and λ, spiral length and pitch; φ_i and φ_0, angular coordinates of the inside endpoint and the outside endpoint of the spiral on its median line; p, pressure; p_i, fluid pressure at the pump inlet; and N, input power.

LITERATURE CITED

1. S. A. Bostandzhiyan, V. I. Boyarchenko, and G. N. Kargopolova, "Flow of a non-Newtonian fluid through the channel of an extruder screw under conditions of complex shear," in: Rheophysics and Rheodynamics of Flow Systems [in Russian], Nauka i Tekhnika, Minsk (1970), pp. 111-121.

AN ARTERIAL HEAT PIPE WITH A GROOVED EVAPORATOR

V. S. Tarasov

UDC 621.565.94

A method is developed for calculating the hydrodynamic heat-transfer boundary of arterial heat pipes with capillary channels having a triangular profile in the evaporator. Comparison with experimental data demonstrates the satisfactory accuracy of the method.

Evaporators for arterial heat pipes (AHP), equipped with ring-shaped capillary channels, e.g., grooves with a triangular profile (V-channels) (Fig. 1), can operate with very dense heat fluxes with high heat-exchange coefficients [1-4]. However, there is no satisfactory theory for calculating the limiting characteristics of such AHP. The difficulty with the hydrodynamic theory developed in [1, 2] is that it does not relate the magnitude of the hydrodynamic heat-transfer boundary (HHTB), which determines the maximum attainable heat flux density in the evaporator, to the pressure losses in the heat carrier in the rest of the AHP and it does not provide a physically correct estimate of the influence of the contact angle on the HHTB.

When heat is input uniformly, all evaporator channels are loaded identically and the HHTB will be determined by the channel in the beginning section of which, for x = 0, the meniscus is curved more strongly than in the neighboring channels [5]. In most cases, this is the edgemost channel that is farthest away from the condensor. For this channel, the following relation is valid:

$$\Delta p_{cap} = \Delta p'_e + \Delta p_{rem} \quad (1)$$

The pressure differential Δp_{rem} in the rest of the AHP causes the meniscus to be curved in the starting section with a radius

$$R_0 = \sigma/\Delta p_{rem}. \quad (2)$$

From the starting section to the end section $x = x_m$, the liquid moves under the action of a capillary pressure gradient, compensating for frictional resistance [1, 2]:

$$\frac{dp'}{dx} = -\frac{dp_{cap}}{dx}. \quad (3)$$

Translated from Inzhenerno-Fizicheskii Zhurnal, Vol. 40, No. 2, pp. 238-243, February, 1981. Original article submitted November 6, 1979.

 0022-0841/81/4002-0138$07.50

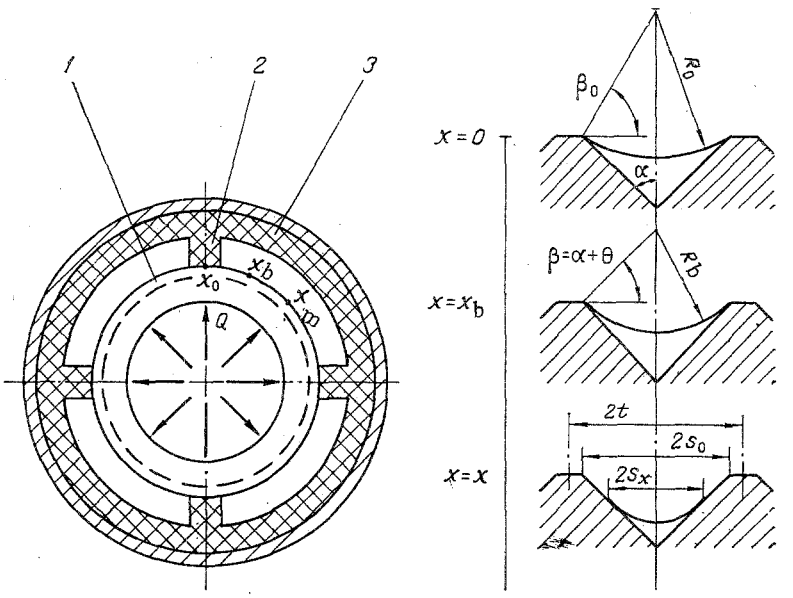

Fig. 1. Computational model for an evaporator with V-channels in AHP: 1) evaporator groove; 2) porous connector; 3) artery.

Assuming that the gradient of the pressure losses due to the friction of the liquid as it undergoes a laminary flow with a linearly decreasing mass flow rate is determined by Poiseuille's law, after integrating (3) taking into account (2), we obtain an equation that determines the maximum heat flux density in the evaporator for isothermal liquid flow in the V-channels (overheating of the liquid is small), when $t > s_0$, $\alpha + \Theta \leq \beta_0 \leq \pi/2$;

$$q_{iso} = \frac{\sigma r}{\nu'} \frac{s_0^3}{x_m^2 t} (2C_1 + C_2), \tag{4}$$

where

$$C_1 = \frac{\sin^2\alpha}{16} \int_{\alpha+\Theta}^{\beta_0} \left(\operatorname{ctg}\alpha + \operatorname{tg}\beta - \frac{\pi/2 - \beta}{\cos^2\beta} \right)^3 \sin\beta d\beta; \tag{5}$$

$$\beta_0 = \arccos(s_0/R_0) = \arccos(s_0 \Delta p_{rem}/\sigma); \tag{6}$$

$$C_2 = \frac{\sin^2\alpha}{24} \left[\operatorname{ctg}\alpha + \operatorname{tg}(\alpha+\Theta) - \frac{\pi/2 - (\alpha+\Theta)}{\cos^2(\alpha+\Theta)} \right]^3 \cos(\alpha+\Theta). \tag{7}$$

The authors of [1, 2] examine the regime $s_{x=0} = s_0$ as a limiting regime for AHP, but the heat pipe is fully operational in cases for which $s_{x=0} < s_0$. Equation (4) in this case takes the form

$$q_{iso} = \frac{\sigma r s_{x=0}^3}{\nu' x_m^2 t} C_2. \tag{8}$$

Thus, the general form for the maximum heat flux density in the evaporator, independent of its operational regime, will be

$$q_{iso} = \frac{\sigma r s_{x=0}^3}{\nu' x_m^2 t} (2C_1 + C_2). \tag{9}$$

For high values of the heat flux density and large overheating of the liquid, although less than ΔT_{low}, changes in the viscosity become significant. This can be taken into account in Eqs. (4), (8), and (9) by a correction in the form of the ratio of the viscosity at the saturation temperature to the viscosity at the average temperature:

$$q_e = q_{iso} \frac{\nu'(T'')}{\nu'(T'' + \Delta T/2)}. \tag{10}$$

Introducing a linear approximation for the temperature dependence of the viscosity

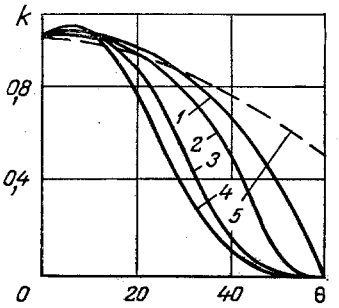

Fig. 2. Influence of the contact angle on HHTB for $\alpha = 30°$: 1) $\beta_0 = 90°$; 2) 78; 3) 60; 4) $\beta_0 = \alpha + \Theta$; 5) $\cos\Theta$.

$$\frac{1}{\nu'(T''+\Delta T/2)} = \frac{1}{\nu'(T'')} + \frac{b}{2}\Delta T \tag{11}$$

and expressing the overheating of the liquid in terms of the heat-exchange coefficient in the evaporator, we obtain

$$q_e = (1/q_{iso} - b\nu'/2\alpha_e)^{-1}. \tag{12}$$

The upper limit in the integral in (5) is determined by pressure losses in the AHP tract to the evaporator according to (6), while the lower limit is determined by the sum of the half angle of the profile and the contact angle. The latter significantly affects the magnitude of both coefficients C_1 and C_2 and the HHTB. Figure 2 shows the dependence of the maximum heat flux density in the evaporator on the contact angle for different initial states of the meniscus $R_0(\Theta = 0) = R_0$ = idem in dimensionless form:

$$k = \frac{q_{iso}(\Theta)}{q_{iso}(\Theta=0)} = \begin{cases} \dfrac{2C_1 + C_2}{2C_1(\Theta=0) + C_2(\Theta=0)} & \text{for } \beta_0(\Theta=0) \geqslant \alpha + \Theta, \\ \dfrac{[\cos^3(\alpha+\Theta)]\,C_2}{(\cos^3\beta_0)[2C_1(\Theta=0)+C_2(\Theta=0)]} & \text{for } \beta_0(\Theta=0) \leqslant \alpha + \Theta. \end{cases} \tag{13}$$

This expression agrees with an analogous dependence presented in [6] for nonarterial heat pipes with longitudinal channels. According to [1, 2], $k = \cos\Theta$, which is valid only for $\alpha = 0$, i.e., for rectangular channels. For triangular channels, the error increases with increasing α and Θ. For $\alpha = 30°$, the accuracy is sufficient for $\Theta \leqslant 15°$, but for $\Theta \to (\pi/2 - \alpha)$ the error becomes large.

It is possible to find the HHTB in AHP with a grooved evaporator analytically only in the particular case when it is known that in the rest of the AHP the flow of both phases is laminary, $s_{x=o} < s_o$ and $g = 0$:

$$q_{iso}(g=0) = \frac{\sigma r}{\nu'}\left\{\frac{C_2}{x_m^2 t}\left[\frac{\cos(\alpha+\Theta)}{f}\right]^3\right\}^{1/4}, \tag{14}$$

where $f = \Delta p_{rem} r/(q_{iso}\nu')$.

If $g \neq 0$, then the explicit expression for HHTB is so cumbersome that it is easier to find it by numerically solving the equation

$$q_{iso} = q_{iso}(g=0)\left(1 \pm \frac{\rho' g h r}{q_{iso}\nu' f}\right)^{-3/4}. \tag{15}$$

In the general case, the HHTB is found by a numerical solution to the system of equations (9) and the hydraulics of the remaining part of the AHP. Figure 3 shows an example of such a calculation for a water AHP, the construction of which is described in [3, 4]. Its evaporator is made of copper and is equipped with an external grooved triangular profile with an apex angle of 60°. The diameter of a groove is 13 mm, the spacing is 0.25 mm, and the width of the channel is 0.2 mm. The artery is connected to the groove at four points, uniformly positioned along a circle so that $x_m = 5.1$ mm. The greatest difference in the levels between the evaporator and the condensor with the AHP in a horizontal position is 22 mm.

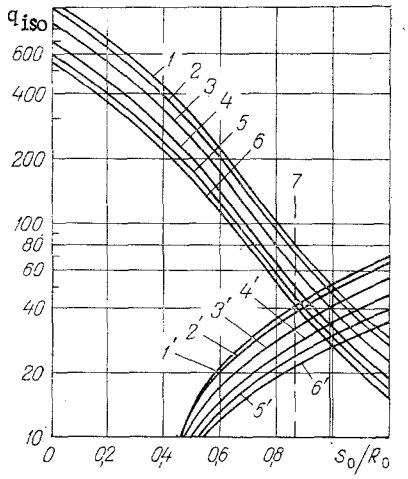

Fig. 3

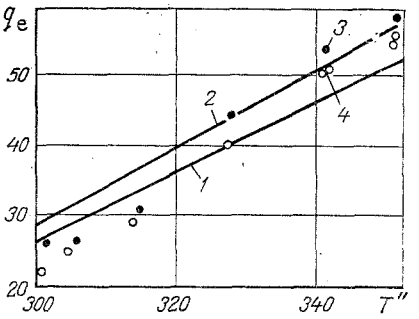

Fig. 4

Fig. 3. Graphical calculation of the maximum heat flux density in AHP with a grooved evaporator operating on water: 1-6) evaporator; 1'-6') remaining part of the AHP; 1, 1') T'' = 351°K; 2, 2') T'' = 343°K; 3, 3') T'' = 328°K; 4,4') T'' = 314°K; 5, 5') T'' = 305°K; 6, 6') T'' = 300°K; 7) $s_0/R_0 = \cos\alpha$. qiso, W/cm^2.

Fig. 4. Comparison of computed and experimental data for water AHP with a grooved evaporator: 1) calculation according to Eq. (15); 2) Eq. (12); experiment: 3) q_e^+; 4) q_e^-.

Using the technique described in [5], we computed the losses of liquid and steam throughout the entire AHP, except the evaporator, with a constant vapor temperature, and based on these, we constructed the curves 1'-6' showing the dependence of the heat flux density in the evaporator as a function of the dimensionless curvature of the meniscus in the starting section of the V-channel. Then, similar relations 1-6 were constructed from Eq. (9) for the same values of the vapor temperature for the evaporator itself. The vertical line 7 is drawn through the boundary value $s_0/R_0 = \cos\alpha$ ($\Theta = 0$). To the left of this line $\beta_0 > \alpha$ and the curves 1-6 were constructed according to (4), and to the right of the line, $\beta_0 = \alpha$ so that the curves were constructed according to (8).

The intersection of the curves 1-6 and 1'-6', corresponding to a single vapor temperature, determines the HHTB for this vapor temperature. The calculations were carried out for temperatures for which experimental data were available. All points of intersection turned out to lie along a single vertical line, i.e., when the HHTB is attained, the curvature of the meniscus at the inlet section of the V-channel did not depend on the vapor temperature. This is explained by the smallness of the losses in vapor pressure for the AHP being examined in comparison with the pressure losses in the liquid (5% for the lowest T''), while the pressure losses in the liquid in the evaporator and in the rest of the AHP obey the same linear law. It is interesting to note that the points of intersection lie to the right of the vertical line 7, i.e., the meniscus in the inlet section of the V-channel is indented ($s_{x=0} < s_0$), and for this AHB, the limiting heat flux can be determined by solving (15).

In Fig. 4 the working points of the HHTB are rewritten in the coordinates T'' – q_e and a second curve is constructed according to (12) taking into account changes in the viscosity of the overheated liquid. In constructing this curve, the coefficient of heat exchange in the evaporator was determined from a slightly modified formula, compared with that proposed in [2]:

$$\alpha_e = 6{,}75\exp(-0{,}0588\alpha^0)\frac{\lambda'}{2t}\frac{R_b}{R_e}\frac{1-43\cdot10^{-6}/2s_0}{2C_1+C_2}. \qquad (16)$$

The modification consists of the fact that in order to take into account the increase in the thermal resistance of a real evaporator, the spacing of the channels and not their width is taken as a characteristic dimension. Figure 4 also shows experimental points, corresponding to normal operation of the evaporator (q_e^-) and overdrying (q_e^+) (experimental setup is described in [3]). The true value of the HHTB must lie between them. The agreement

between the experimental and computed values of HHTB is very good for high heat flux densities (exceeding 40 W/cm^2); it is somewhat worse for smaller values, for which the experimental points are lower by 10-20%. Probably, this is explained by the increase in the relative heat losses in the experimental setup with a decrease in the power transmitted in the AHP.

The overheating of the evaporator wall measured in the experiment was not used in constructing the curve 2 in Fig. 4, since the overheating was quite high: the thermocouples, measuring the temperature of the evaporator wall, were placed on its outer face on the inlet side of the heat source and the face was cooled only by heat conduction to the working region, on which there was a groove. The accuracy of the measurement of the wall temperature had no particular significance for establishing the onset of HHTB. Nevertheless, even strongly underestimated values of the heat exchange coefficients in the evaporator, computed according to the measured overheating of its endface, are quite impressive: from 20,000 to 28,000 W/m^2·K. A calculation based on formula (16) gives, for these conditions, 37,200 W/m^2·K.

It was impossible to establish in the experiments the presence or absence of boiling of the water in the groove of the evaporator. It was only possible to present indirect proof for its absence. The noise associated with bubbles could not be heard. And, most important, overheating of the water was not enough for boiling. In [2], the overheating of the water, necessary for onset of boiling in a copper groove with T" = 366°K in the region q_e = 50-80 W/cm^2, is determined in the range 22-23°K. The greatest overheating of the water in the experiments could not be greater than 17.5°K for T" = 351°K. If the fact that the distilled water in the AHP was carefully degassed is taken into account, then it must be acknowledged that there is much evidence in support of the absence of boiling.

NOTATION

g, acceleration of gravity, m/sec^2; h, distance along the vertical between the edgemost faces of the evaporator and the condensor, m; $\Delta p'_e$, pressure differential in the liquid in the evaporator, N/m^2; Δp_{rem}, pressure differential in the heat carrier in the rest of the AHP with the exclusion of the evaporator, N/m^2; Δp_{cap}, moving capillary potential for circulation of the heat carrier, N/m^2; q_{iso}, heat flux density in the evaporator for isothermal liquid flow, W/m^2; q_e, heat flux density taking into account overheating of the fluid, W/m^2; R_b, radius of the heat inlet surface, m; R_e, radius of the working evaporator surface, m; r, heat of vaporization, J/kg; $2s_x$, width of the meniscus of the liquid in the x-section, m; $2s_o$, width of the channel, m; 2t, spacing of the channels, m; T", saturation temperature, vapor temperature, °K; ΔT, overheating of the liquid relative to T", °K; x, coordinate along the channel axis, m; x_m, maximum distance for transport of fluid in the channel, m; 2α, angle of the channel profile; α_e, heat-exchange coefficient in the evaporator, W/m^2·K; λ, coefficient of thermal conductivity, W/m·K; ν, kinematic viscosity coefficient, m^2/sec; ρ, density, kg/m^3; σ, coefficient of surface tension, N/m. The indices are as follows: ', liquid; and ", vapor.

LITERATURE CITED

1. Morits, "Influence of the capillary geometry on the maximum heat load in heat pipes," in: Heat Pipes [Russian translation], É. É. Shpil'rain (ed.), Mir, Moscow (1972), p. 33.
2. K. T. Feldman and M. E. Berger, "Analyses of a high heat flux water heat pipe evaporator," Technical Report ME-62 (73) ONR-012-2. The University of New Mexico, Albuquerque, New Mexico (1973).
3. V. G. Voronin, A. V. Revyakin, and V. S. Tarasov, "Development and investigation of a heat pipe for cooling a high-power electron-vacuum device," in: Problems in Radioelectronics [in Russian], Yu. E. Spokoinyi (ed.), Ser. TRTO (1974), No. 2, p. 21.
4. V. G. Voronin, A. V. Revyakin, V. Ya. Sasin, and V. S. Tarasov, Low-Temperature Heat Pipes for Aircraft [in Russian], G. I. Voronin (ed.), Mashinostroenie, Moscow (1976).
5. V. S. Tarasov, "Hydrodynamic limit for heat transfer in branching heat pipes," in: Extreme Cold and Conditioning [in Russian], G. I. Voronin (ed.), Tr. MVTU im. Baumana (1976), No. 240, p. 136.
6. V. Ya. Sasin, B. R. Temkin, and A. I. Arkhipov, "Mass and heat transfer processes in channelled nonarterial heat pipes," in: Problems in Heat Transfer [in Russian], A. I. Leont'ev, P. M. Brdlika, and V. P. Motulevich (eds.), Forestry Institute, Moscow (1976), p. 159.